

Increased Proliferative Cells in the Medullary Thick Ascending Limb of the Loop of Henle in the Dahl Salt-Sensitive Rat

Chun Yang, Francesco C. Stingo, Kwang Woo Ahn, Pengyuan Liu, Marina Vannucci, Purushottam W. Laud, Meredith Skelton, Paul O'Connor, Terry Kurth, Robert P. Ryan, Carol Moreno, Shirng-Wern Tsaih, Giannino Patone, Oliver Hummel, Howard J. Jacob, Mingyu Liang, Allen W. Cowley Jr

Abstract—Studies of transcriptome profiles have provided new insights into mechanisms underlying the development of hypertension. Cell type heterogeneity in tissue samples, however, has been a significant hindrance in these studies. We performed a transcriptome analysis in medullary thick ascending limbs of the loop of Henle isolated from Dahl salt-sensitive rats. Genes differentially expressed between Dahl salt-sensitive rats and salt-insensitive consomic SS.13^{BN} rats on either 0.4% or 7 days of 8.0% NaCl diet (n=4) were highly enriched for genes located on chromosome 13, the chromosome substituted in the SS.13^{BN} rat. A pathway involving cell proliferation and cell cycle regulation was identified as one of the most highly ranked pathways based on differentially expressed genes and by a Bayesian model analysis. Immunofluorescent analysis indicated that just 1 week of a high-salt diet resulted in a severalfold increase in proliferative medullary thick ascending limb cells in both rat strains, and that Dahl salt-sensitive rats exhibited a significantly greater proportion of medullary thick ascending limb cells in a proliferative state than in SS.13^{BN} rats (15.0±1.4% versus 10.1±0.6%; n=7–9; *P*<0.05). The total number of cells per medullary thick ascending limb section analyzed was not different between the 2 strains. The study revealed alterations in regulatory pathways in Dahl salt-sensitive rats in tissues highly enriched for a single cell type, leading to the unexpected finding of a greater increase in the number of proliferative medullary thick ascending limb cells in Dahl salt-sensitive rats on a high-salt diet. (*Hypertension*. 2013;61:208-215.) • [Online Data Supplement](#)

Key Words: kidney ■ gene expression ■ cell cycle

Gene or protein expression profiles have been studied in whole organs or partial organs collected from various animal models of hypertension. Examples include analysis of cardiac and renal transcriptomes in the spontaneously hypertensive rat, the Lyon hypertensive rat, and the Dahl salt-sensitive (SS) rat.^{1–3} The SS rat is a well-established model of human salt-sensitive hypertension and renal injury. The consomic SS.13^{BN} rat was derived by substituting Brown Norway chromosome 13 into the SS genome. Salt-induced hypertension and renal injury were substantially attenuated in the SS.13^{BN} rat.⁴ Our analysis of the transcriptomes and proteomes in the renal medulla and the renal cortex of SS and SS.13^{BN} rats has revealed several novel mechanisms and partial regulatory networks that may contribute to the development of hypertension or renal injury in the SS rat.^{5–10} The novel mechanisms discovered include those involving fumaric acid metabolism and renal 11 β -hydroxysteroid dehydrogenase type 1.^{11–13}

Cell type heterogeneity, however, has been a significant hindrance in the interpretation of these studies. The renal cortex and the renal medulla contain epithelial, connective, and vascular tissues. Each tissue includes multiple cell types. For example, the nephron epithelia consist of several segments, each with unique physiological and molecular characteristics. Differential expression between animals may in some cases reflect differences in cellular composition of the tissue being analyzed rather than expression changes in a given cell type. Dominant cell types may prevent detection of important changes in gene expression taking place in a minority cell type.

In the present study, we performed a transcriptome analysis in medullary thick ascending limbs (mTALs) of the loop of Henle isolated from SS rats and SS.13^{BN} rats. The mTAL is highly relevant to the pathophysiological mechanisms of hypertension, especially in the SS rat.^{14–26}

Received May 24, 2012; first decision June 12, 2012; revision accepted October 18, 2012.

From the Department of Physiology (C.Y., P.L., M.S., P.O., T.K., R.P.R., C.M., H.J.J., M.L., A.W.C.), Division of Biostatistics (K.W.A., P.W.L.), Cancer Center (P.L.), Human and Molecular Genetics Center (C.M., S.-W.T., H.J.J.), and Cardiovascular Center (A.W.C.), Medical College of Wisconsin, Milwaukee, WI; Department of Biostatistics, MD Anderson Cancer Center, Houston, TX (F.C.S.); Department of Statistics, Rice University, Houston, TX (M.V.); and Max-Delbrück-Center, Berlin, Germany (G.P., O.H.).

The online-only Data Supplement is available with this article at <http://hyper.ahajournals.org/lookup/suppl/doi:10.1161/HYPERTENSIONAHA.112.199380/-/DC1>.

Correspondence to Mingyu Liang or Allen W. Cowley Jr, Medical College of Wisconsin, 8701 Watertown Plank Rd, Milwaukee, WI 53226. E-mail mliang@mcw.edu or cowley@mcw.edu

© 2012 American Heart Association, Inc.

Hypertension is available at <http://hyper.ahajournals.org>

DOI: 10.1161/HYPERTENSIONAHA.112.199380

We applied a new method of pathway analysis using a Bayesian modeling approach that incorporated previous knowledge of biological pathways and was independent of any a priori determination of differential expression.²⁷ The study led to an unexpected discovery that mTALs in SS rats on a high-salt diet exhibited increased proliferative activities.

Methods

See the online-only Data Supplement for a detailed Methods section.

Animals

Male SS and consomic SS.13^{BN} rats were generated and maintained as described.^{4,8} Rats were studied at 6 weeks of age while maintained on a 0.4% salt diet (AIN-76A, Dyets) or at 7 weeks of age after 1 week of an 8.0% salt diet. The time points represent an early stage of the development of hypertension.⁸

Isolation of mTALs

mTALs were isolated using a bulk dissection method as described previously with modifications.^{18,28}

Tamm-Horsfall Protein Staining

Samples of isolated mTALs were stained with antibody against Tamm-Horsfall protein.

RNA Extraction

RNA was extracted as described⁸ and assessed by Agilent BioAnalyzer 2100 and spectrophotometry.

Real-Time Polymerase Chain Reaction

Real-time polymerase chain reaction (PCR) analysis of selected mRNAs was performed using the SYBR Green chemistry (Table S1 in the online-only Data Supplement).^{8,29}

Affymetrix Expression Array Analysis

Affymetrix Rat Expression Array 230 2.0 was hybridized following the manufacturer's protocols.⁸ Sixteen arrays were used to analyze 2 rat strains and 2 salt conditions (0.4% and 7 days of 8.0%) with 4 individual samples in each experimental group. Signal intensities were normalized by robust multiarray average expression measure. Differentially expressed genes were identified by rank-product methods. Ingenuity pathway analysis was used for pathway analysis.⁸

Chromosomal Representation Index

Representation of a chromosome in differentially expressed genes was calculated as we have described previously.⁷

Bayesian Model Analysis

A pathway-based analysis was performed using a modified version of the Bayesian model described recently.²⁷ The Bayesian method integrates pathway information with the experimental data to identify pathways and genes related to a binary phenotype. Briefly, we used the Kyoto Encyclopedia of Genes and Genomes (<http://www.genome.jp/kegg/>) to retrieve an S matrix indicating memberships of genes to pathways and an R matrix describing relationships between genes within and between pathways. The matrices were used to define probability distributions of pathways and genes, called priors. A Monte Carlo Markov chain algorithm was applied to explore the posterior space efficiently and to find the most probable configurations of genes and pathways. The procedure results in a list of visited models with included pathways and genes and their corresponding relative posterior probabilities. The posterior probability represents the likelihood of a pathway or gene to discriminate 2 experimental groups.

Defining Boundaries of Congenic Segments Using Single Nucleotide Polymorphism Arrays

We previously identified 4 nonoverlapping congenic regions on rat chromosome 13 that had significant effects on hypertension in the SS rat, designated as lines 1, 5, 9, and 26.³⁰ In the present study, we obtained precise boundaries for lines 5, 9, and 26 using the RATDIVm520813 single nucleotide polymorphism array (803484 single nucleotide polymorphisms genome wide).

Immunofluorescence Analysis of Cell Proliferation

Proliferative cells were identified by positive staining of Ki-67. Cells in the G₂/M phases were identified by positive staining of histone H3 phosphorylated at Ser10 (p-H3 or H3-P). Cell nucleus was visualized by 4'-6-diamidino-2-phenylindole staining. Ten fields were randomly selected from each kidney. mTALs were identified by morphology. The numbers of all cells (cell nuclei), Ki-67-positive cells, and H3-P-positive cells within mTALs were manually counted. The investigator analyzing the images was blinded to the treatment conditions of the rats.

Terminal Deoxynucleotidyl Transferase-Mediated dUTP Nick End Labeling

Terminal deoxynucleotidyl transferase-mediated dUTP nick end labeling staining of kidney sections was performed using the DeadEnd Fluorometric TUNEL System from Promega following the manufacturer's instructions.

Statistical Analysis

Affymetrix array data were analyzed as described above. Data from other experiments were analyzed using the Student *t* test or ANOVA and reported as mean±SEM. *P*<0.05 was considered significant.

Results

Quality Control of mTAL Isolation and RNA Extraction

More than 100 SS or SS.13^{BN} rats were used for mTAL isolation and RNA extraction. Samples from 16 rats were selected for Affymetrix expression array analysis based on substantial enrichment of mTALs, high RNA quality, and sufficient RNA amounts.

Enrichment of mTALs was assessed by real-time PCR quantification of Na-K-2Cl cotransporter, a marker of thick ascending limbs; aquaporin 1, a marker of proximal tubules; aquaporin 2, a marker of collecting ducts; urea transporter B, a marker of descending Vasa recta; and plasmalemma vesicle protein 1, a marker of endothelial cells. Compared with renal outer medulla tissues, the ratio of Na-K-2Cl cotransporter abundance to each of the other marker genes was substantially increased in isolated mTALs, indicating a 4- to 7-fold enrichment of mTALs relative to other nephron and vascular segments (Figure 1A). The purity of mTAL isolations was further assessed by staining of Tamm-Horsfall protein, a protein specifically expressed in mTALs (Figure 1B). From 600 tubular segments in 10 images from 3 isolations, we determined that 93.2% of the segments were mTALs.

All 16 of the samples had RNA integrity numbers >8.5 (Figure 1C), 260/280 nm ratios of 1.9 to 2.0, and a total amount of RNA >4 μg.

Differentially Expressed Genes

Of 31 099 expressed sequence tag probe sets on the Affymetrix expression array, 14 677 were considered detectable in all of

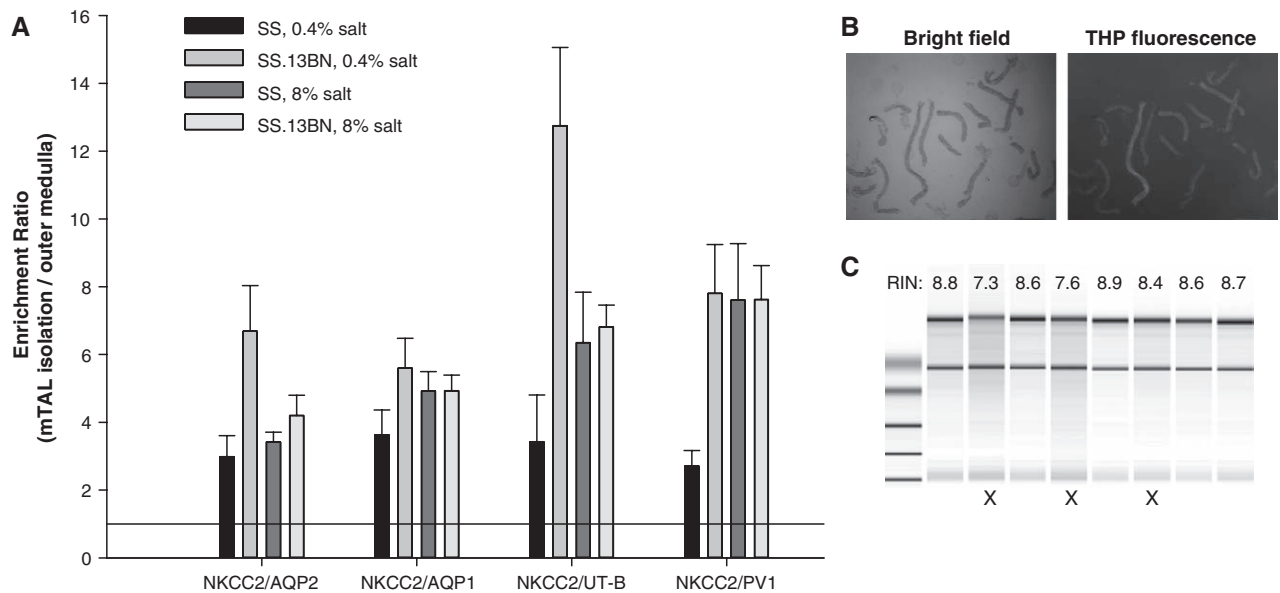


Figure 1. Quality control of medullary thick ascending limb (mTAL) isolation and RNA extraction. **A**, Real-time polymerase chain reaction (PCR) analysis of marker genes. Enrichment of mTALs in the mTAL isolations vs the outer medulla was assessed by examining abundance ratios of an mTAL marker (Na-K-2Cl cotransporter [NKCC2]) to markers of other cells (see Results section). The ratios were artificially set as 1 for the outer medulla. **B**, The majority of the collected nephron segments (bright field) were stained positive for Tamm-Horsfall protein (THP), an mTAL-specific protein. **C**, Bioanalyzer analysis of RNA samples. Samples marked with X were discarded.

the mTAL samples. Rank-product analysis identified 217 and 291 expressed sequence tags as differentially expressed between SS and SS.13^{BN} rats on 0.4% salt and 7 days of 8.0% salt, respectively, based on the criteria of false discovery rate <0.05 and \log_2 ratio >0.5 or ≤ 0.5 . The differentially expressed sequence tags and associated gene annotations are shown in Table S2.

Real-time PCR was performed to analyze 3 and 16 of the genes differentially expressed on 0.4% and 8.0% salt diets, respectively, as well as 2 genes not considered differentially expressed on the 0.4% salt diet. Several of the genes analyzed by quantitative PCR, including *Cdc73*, *Cdc2*, *Cenpf*, *E2f8*, and *Elk4*, are involved in cell cycle regulation, a pathway that we chose to focus on in the later part of the current study. Real-time PCR was done in the samples used in the Affymetrix expression array study, as well as several additional mTAL samples. Nine of the 19 cases of differential expression were confirmed statistically (Figure S1 in the online-only Data Supplement). Four cases (*Il1b*, *Elk4*, *Dars2*, and *Col1a1[LS]*) approached statistical significance (*P* values between 0.05 and 0.10). The remaining 6 cases had *P* values >0.1 but were still directionally consistent with the array data, although some of them showed smaller fold changes than the array data suggested.

Genes differentially expressed in mTALs between SS and SS.13^{BN} rats were highly enriched for genes located on chromosome 13, the chromosome substituted in SS.13^{BN} (Figure 2). The representation index for genes on chromosome 13 was 6.7 and 4.4 on 0.4% and 8.0% salt diets, respectively, compared with an average of 1.1 for all chromosomes. Several of the differentially expressed genes located on chromosome 13 fall in the 4 nonoverlapping congenic regions that we identified previously as having significant effects on hypertension in the SS rat (Table S2).³⁰ The genomic boundaries of 3 of the

4 congenic regions were newly defined using a rat single nucleotide polymorphism array analysis (Table S3). Several of the genes chosen for real-time PCR verification are located in these congenic regions. These included *Elk4* and *Slc45a3* in the line 5 region, *Plekha6* and *Golt1a* in line 9, and *Fam129a* and *Dars2* in line 26.

Ingenuity Pathway Analysis

Ingenuity pathway analysis of the genes differentially expressed between SS and SS.13^{BN} rats identified several canonical pathways as highly represented. The top 10 pathways identified at each salt diet condition were listed in Table S4. The top 5 pathways identified on the 8% salt diet were hepatic fibrosis/hepatic stellate cell activation, mitotic roles of polo-like kinase, atherosclerosis signaling, cell cycle G₂/M DNA damage checkpoint regulation, and ataxia telangiectasia-mutated gene signaling.

Note that the name of a canonical pathway may be uninformative or even misleading in some cases. For example, the hepatic fibrosis pathway includes elements of fibrosis in general and should not be considered irrelevant to the kidney tissue. Similarly, the atherosclerosis signaling pathway involves several elements of inflammation and fibrosis that are applicable to nonvascular tissues. The ataxia telangiectasia-mutated gene signaling pathway is involved in the regulation of DNA repair, the cell cycle, and apoptosis.

Pathways and Genes Identified by the Bayesian Model Analysis

Ingenuity pathway analysis nominates pathways based on enrichment of differentially expressed genes. It does not take into account detailed patterns of changes in mRNA abundance or biological relationships known to exist among genes.

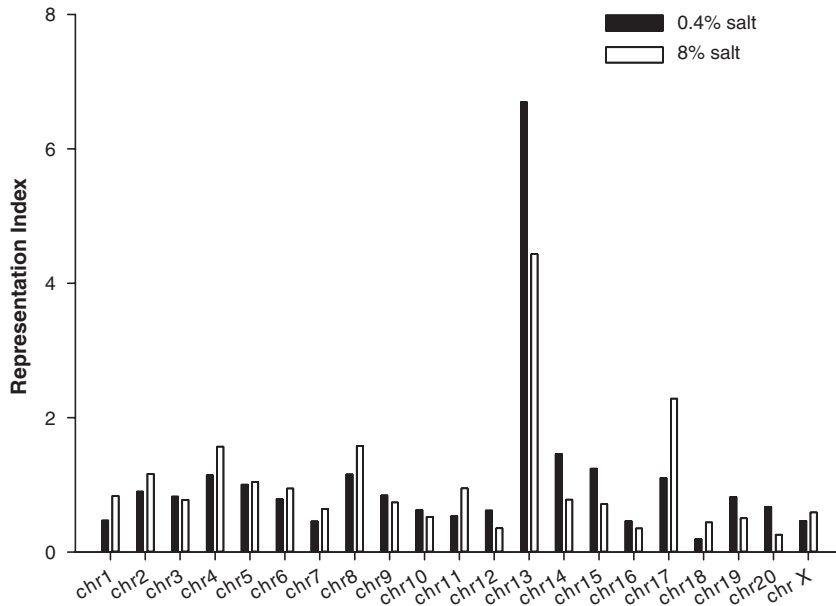


Figure 2. Genes differentially expressed in medullary thick ascending limbs (mTALs) between Dahl salt-sensitive (SS) and SS.13^{BN} rats were enriched for genes located on chromosome 13. See the online-only Supplemental Methods section for an explanation of how the representation index was calculated.

Differential expression is typically determined by arbitrary criteria, the limitations of which are exacerbated by the small number of replicates in a typical gene expression profiling study.

We therefore performed a Bayesian model analysis to identify biological pathways and genes that were best at discriminating the 2 rat strains. The Bayesian analysis was performed without a priori determination of differential expression. The intensity of gene expression was directly used in the model to nominate pathways and genes. Moreover, the Bayesian analysis considered known relationships among genes.

A total of 2781 genes were included in the Bayesian model analysis. These genes were selected because they exhibited variations among samples and were members of ≥ 1 of the 244 pathways in the Kyoto Encyclopedia of Genes and Genomes pathway database. Variations among samples were assessed by a K-means clustering algorithm³¹ (K=6) applied to the SD of each gene among the samples. The Table shows the pathways with posterior probability >0.5 in the comparison of SS and SS.13^{BN} rats on the 8% NaCl diet. Also shown in the Table are member genes of a pathway that had posterior probability >0.5 given the set of selected pathways and were ranked in the top 10 genes within the pathway. Pathways and genes identified on the 0.4% NaCl diet are shown in Table S5. Note that the Bayesian analysis does not unequivocally exclude a pathway or a gene. The analysis ranks pathways or genes by their posterior probabilities, and the ranking is more informative than absolute values of posterior probability.

We assessed whether expression data and known relationships among genes (the R matrix) both contributed to the ranking of pathways. Pathways were ranked based on posterior probabilities obtained from analyses considering expression data only or both expression data and the R matrix. Analysis incorporating the R matrix generally yielded higher posterior probabilities. The assessment, however, focused on the ranking of pathways. The correlation of pathway rankings under the 2 analytical conditions was plotted in Figure 3. The spread of the plot (deviations from the line of identity) suggests that known relationships among genes contributed to the ranking.

The high degree of correlation, on the other hand, suggests that expression data or other properties of the pathways, such as pathway size, contributed importantly to the ranking of pathways. As expected, there was a correlation between pathway size and posterior probability. However, there were also pathways of the same size that had very different posterior probabilities. Therefore, it appears that, although larger pathways had a higher probability to be selected, it was necessary that the data supported the selection.

Increased Proliferative Cells in mTALs of SS Rats on the 8% Salt Diet

A cell cycle pathway was one of the most highly ranked pathways according to the Ingenuity Pathway Analysis of genes differentially expressed between SS and SS.13^{BN} rats on the 8% salt diet (Table S4). A pathway titled Pathways in Cancer, which is largely related to cell cycle and proliferation regulation, was one of the most highly ranked pathways according to the Bayesian model analysis (Table). Based on this prediction, we performed studies to specifically examine the status of cell proliferation in mTALs in SS and SS.13^{BN} rats.

As shown in Figure 4, 2.3% to 4.4% of all mTAL cells were in a proliferative state (positive for Ki-67 staining) when the rats were on the 0.4% salt diet (not significantly different between SS and SS.13^{BN} rats). Exposure to the 8.0% salt diet for 7 days substantially increased the number of proliferative mTAL cells in both strains. In SS rats on the 8.0% salt diet, 15.0% of mTAL cells analyzed were in a proliferative state, which was significantly higher than the 10.1% in SS.13^{BN} rats (n=7–9; $P<0.05$; Figure 4).

Despite a higher proportion of cells that were in a proliferative state, SS rats did not have more total cells in each mTAL section analyzed compared with SS.13^{BN} rats. The total number of cells per mTAL section analyzed was 11.6 in SS rats on the 8% salt diet, which was not significantly different from 10.7 cells per mTAL section in SS.13^{BN} rats (n=7–9; Figure 4). The number of mTAL sections analyzed was lower in SS rats on the 8% NaCl diet than in SS.13^{BN} rats (24.4 \pm 1.3 versus 33.0 \pm 1.6 mTAL

Table. Top Pathways (Posterior Probability >0.5) and Top Genes Given Pathways Identified by Bayesian Model Analysis of Data From Rats Fed the 8% NaCl Diet

pathway_id	pathway_names	Posterior Probability	Top 10 Genes With Posterior Probability >0.5 and in Order of Ranking
hmr04144	Endocytosis	1.0000	Igf1r, Pdgfra, Hras, Egfr, Met, Src, Cblb, Kdr, Kit, Flt1
hmr04010	MAPK signaling pathway	1.0000	Mapk1, Mapk3, Kras, Pdgfra, Nras, Hras, Egfr, Prkca, Prkcb, Mapk12
hmr04080	Neuroactive ligand-receptor interaction	0.8848	Grm2, Gabbr1
hmr05200	Pathways in cancer	0.7966	Pik3cd, Pik3r1, Pik3r2, Pdgfra, Mapk1, Kras, Pik3r3, Pik3ca, Igf1r, Mapk3
hmr04062	Chemokine signaling pathway	0.6943	Gnai2, Pik3cd, Pik3r2, Pik3ca, Pik3r1, Pik3r3, Mapk1, Mapk3, Gnai3, Gnai1
hmr04060	Cytokine-cytokine receptor interaction	0.6521	Pdgfra, Egfr, Met, Kdr, Flt1, Kit, Csf1r, Il2rg, Vegfc, Flt4
hmr04910	Insulin signaling pathway	0.6111	Pik3cd, Pik3r2, Mapk1, Pik3r1, Pik3r3, Nras, Kras, Pik3ca, Pik3cb, Mapk3
hmr04141	Protein processing in endoplasmic reticulum	0.5987	Mapk10, Mapk9
hmr03013	RNA transport	0.5522	(none)

The pathways and genes were identified as being best able to discriminate SS and SS.13^{BN} rats fed the high-salt diet. See the Methods section for details.

sections per field; $n=7-9$; $P<0.05$), likely because mTALs with overt damage, which were more prevalent in SS rats, were not included in the counting because it was difficult to obtain accurate cell counts from damaged segments.

The number of cells that were in the G₂/M phases (positive for p-H3 staining) was very small in all of the treatment groups. The number tended to be higher in SS rats on the 8% salt diet (0.60 ± 0.20 cells per field) than in SS.13^{BN} rats (0.28 ± 0.13 cells per field), but the difference did not reach statistical significance. The p-H3 staining procedure appeared to have worked properly, because a significant number of cultured HeLa cells stained positive (Figure S2), although we could not directly compare staining in cultured cells and kidney sections.

In SS rats on the high-salt diet, $0.68\pm 0.36\%$ of cells in morphologically normal mTAL segments stained positive in the terminal deoxynucleotidyl transferase-mediated dUTP nick end labeling analysis of apoptosis, which tended to be higher than in SS.13^{BN} rats ($0.11\pm 0.05\%$), but the difference did not reach statistical significance. The proportions of positive cells were $0.23\pm 0.19\%$ in SS rats and $0.15\pm 0.06\%$ in SS.13^{BN} rats on the 0.4% salt diet (not significantly different).

Discussion

The present study was the first to characterize the transcriptome in a specific nephron segment in a model of hypertension and one of the first to study the transcriptome in tissues highly enriched for a single cell type in hypertension. Transcriptome

analyses have been reported in nephron segments isolated from humans or animal models under physiological conditions.³²⁻³⁵ The mTAL is particularly relevant to the SS rat model of hypertension. Impairment of pressure natriuresis in SS rats has been attributed to elevated NaCl reabsorption in the loop of Henle.^{19,25} Dopamine and nitric oxide inhibit Na⁺/K⁺-ATPase activity or chloride reabsorption in the thick ascending limb less effectively in SS rats than in Dahl salt-resistant rats.^{21,22} Production of 20-hydroxyeicosatetraenoic acid, which inhibits chloride transport in mTALs, is diminished in mTALs in SS rats.^{18,26} Na-K-2Cl cotransporter, which mediates the bulk of NaCl reabsorption in the thick ascending limb, is upregulated in SS rats and possibly in humans with elevated blood pressure salt sensitivity.¹⁴⁻¹⁷ mTALs contribute to increased production of reactive oxygen species in SS rats, which may contribute to the impairment of medullary blood flow regulation that is important for pressure natriuresis.^{20,23,24}

In the differentially expressed genes involved in the identified Ingenuity canonical pathways, Cxcr4, F5, Fcgr3a, Pla2g4a, and Ptgs2 are located on rat chromosome 13. These genes are involved in inflammation, fibrosis, and arachidonic acid metabolism, which are known to contribute to or exacerbate the development of hypertension. Much more work, however, would need to be done before any causal contribution of these genes to hypertension could be established. Importantly, differentially expressed genes not mapped to the consomic chromosome could still be highly relevant to the hypertension phenotype. It is unlikely that

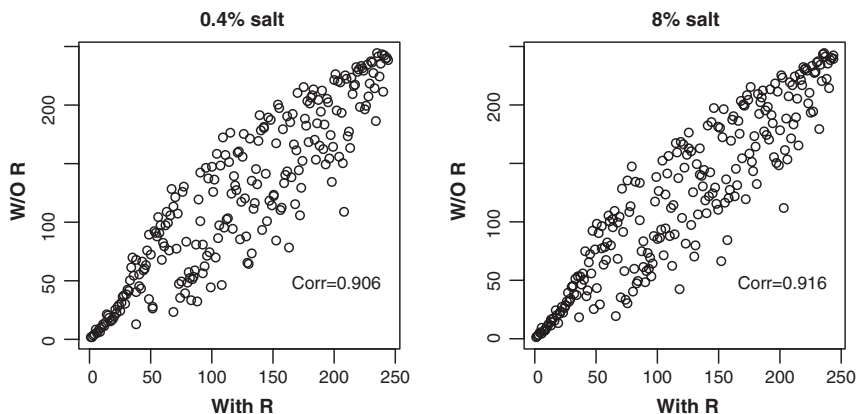


Figure 3. Both existing knowledge of gene-gene relationships and the expression profile data contributed to the ranking of pathways in the Bayesian analysis. Rankings of 244 pathways were plotted. A higher ranking indicates that the pathway is more likely to discriminate the 2 rat strains. R indicates R matrix describing known relationships between genes.

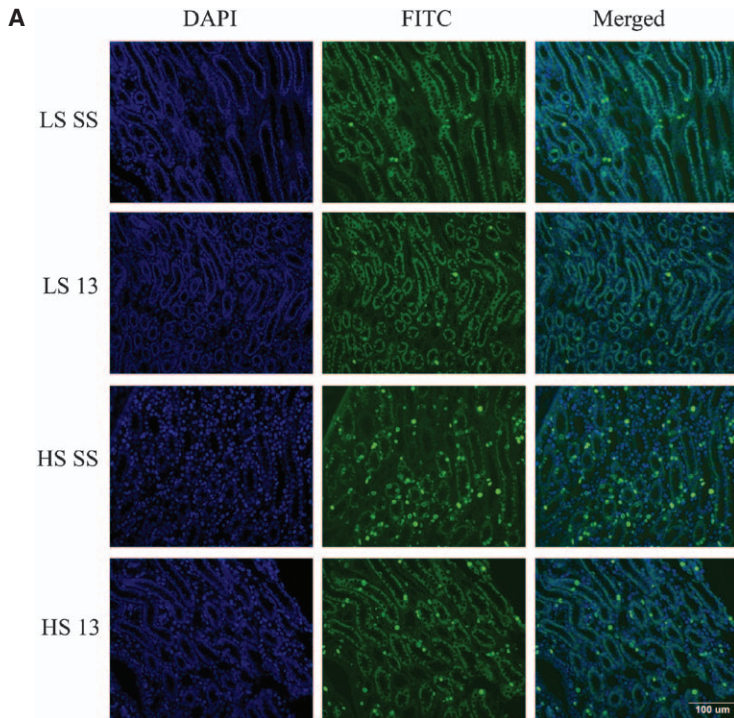
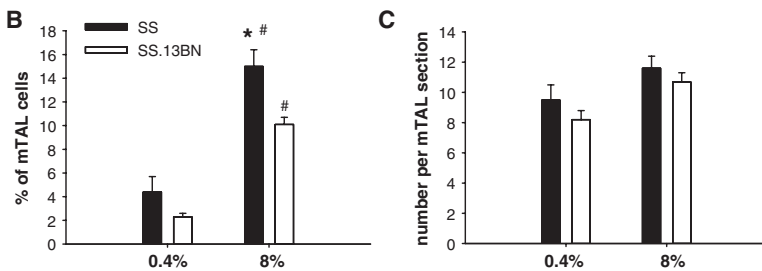


Figure 4. More medullary thick ascending limb (mTAL) cells were in a proliferative state in Dahl salt-sensitive (SS) rats on the 8% salt diet than in SS.13^{BN} rats. LS indicates 0.4% NaCl diet; HS, 8% NaCl diet for 7 days; 13, SS.13^{BN} rats. n=4 for LS groups, n=7 to 9 for HS groups. *P<0.05 vs SS.13^{BN} on HS; #P<0.05 vs LS of the same strain.



causal genes located on the consomic chromosome are the only genes involved in the development and progression of the hypertension phenotype. Instead, it is likely that the causal genes contribute to the hypertension phenotype by influencing, directly or indirectly, biological pathways involving genes located on other chromosomes, forming a tree-like regulatory network that we proposed previously.¹¹

We performed previously a transcriptome analysis of the renal outer medulla, using the same rat strains, dietary conditions, and array platform as the current study of mTALs.⁸ Several inflammation-related pathways were identified as highly represented in the differentially expressed genes by Ingenuity Pathway Analysis in both studies. Some pathways, however, were identified in only 1 of the 2 studies. For example, β -adrenergic signaling and nitric oxide signaling pathways were identified only in the outer medulla study, whereas pathways related to fibrosis and cell cycle regulation were identified only in the mTAL study.

A novel and unexpected finding of the current study was that SS rats fed the high-salt diet had more mTAL cells that were in a proliferative state compared with SS.13^{BN} rats. Moreover, the high-salt diet increased proliferative mTAL cells by severalfold in both strains of rats. The majority of terminally differentiated cells in the kidney, including mTAL cells, are in the quiescent

state of G₀. Proximal tubular cells can re-enter the cell cycle after massive cell death that occurs in conditions such as severe ischemic-reperfusion injury.³⁶ However, even in ischemic-reperfusion injury, mTALs are largely spared. It is, therefore, rather unexpected that we found increased proliferative mTAL cells in rats fed the high-salt diet, especially SS rats. Interestingly, alterations of cell cycle regulation in the kidneys of SS rats were suggested not only by the current mTAL transcriptome analysis but also by our previous transcriptome analysis of the renal cortex.⁸ The cell cycle regulation pathway, however, was not identified in the analysis of homogenized renal outer medulla tissue.⁸ In the current mTAL study, the cell cycle regulation pathway was prominent in strain comparisons under both 0.4% and 8.0% salt conditions according to the Bayesian analysis, and the top 10 ranking genes largely overlapped. However, SS rats on the 0.4% salt diet did not show a significant difference in mTAL proliferative states compared with SS.13^{BN} rats. The ranking of the top genes differs between the 2 dietary salt conditions. Expression patterns for some of the specific genes also differ between the 2 conditions. In addition, Ingenuity Pathway Analysis identified cell cycle-related pathways from the high-salt data set only.

It remains to be determined what mechanisms cause the increase in proliferative mTAL cells in SS rats on the

high-salt diet. Angiotensin II, at doses that do not increase proliferation of proximal tubular cells, stimulates proliferation of a murine mTAL cell line via angiotensin II type 1 receptors.³⁷ The SS rat is a low-renin model of hypertension. However, intrarenal levels of angiotensin II have been shown to be abnormally high in SS rats fed a high-salt diet.^{38,39} In addition, reactive oxygen species at moderate concentrations can stimulate cell proliferation.^{40,41} The renal medulla of SS rats is known to have higher levels of reactive oxygen species, including superoxide and H₂O₂ compared with SS.13^{BN} rats, which contributes to the development of hypertension in SS rats.^{42,43}

The nature of the cell cycle alteration that we observed and its functional consequences remain to be investigated. Nevertheless, the current study has provided several interesting clues. Despite increased proliferative mTAL cells in SS rats, total cells per mTAL section were not significantly different between SS and SS.13^{BN} rats. In fact, total cells per mTAL section were not significantly different between rats on the 2 salt diets, although proliferative mTAL cells increased by severalfold in rats fed the high-salt diet. There are 2 possible explanations. One, mTAL cells were proliferating to replace lost cells. Two, the proliferative mTAL cells had exited G₀ but were not able to progress through the cell cycle to complete cell division. SS rats fed the high-salt diet had more mTALs that were overtly damaged and filled with casts, as one would expect. However, we only counted cells in mTALs that appeared normal because cells in damaged mTALs were distorted, making it difficult to obtain accurate counts. Therefore, it appears that the more likely scenario is that proliferative mTAL cells were arrested at some point of the cell cycle.

G₂/M arrest of proximal tubular cells after injury contributes to the development of tubulointerstitial fibrosis.³⁶ Tubulointerstitial fibrosis in the outer medullary region is a pathological hallmark of SS rats and is significantly attenuated in SS.13^{BN} rats.^{4,9} It would be consistent with the fibrotic phenotype if proliferative mTAL cells in SS rats were arrested in G₂/M. SS rats on the high-salt diet indeed tended to have more mTAL cells that were in G₂/M phases. However, very few mTAL cells overall were in G₂/M phases in either strain of rats on either salt diet. This suggests that the proliferative mTAL cells that we observed might be in the G₁ or S phase. G₁/S arrest can be a response to mild DNA damage, allowing DNA repair to take place.^{44,45} Failure of repair could lead to apoptosis. Apoptosis appears to increase in the injured kidneys of SS rats,⁴⁶ although we were not able to detect a significant difference in apoptotic cells in morphologically normal mTALs between SS and SS.13^{BN} rats. A proinflammatory milieu, which exists in the kidneys of SS rats,^{38,47} could also cause G₁/S arrest.⁴⁸

It remains to be determined whether the signal that stimulates mTAL cell proliferation in SS rats is the same signal that prevents mTAL cells from completing the cell cycle. Cellular signals for proliferation and G₁/S arrest are often distinct. For example, reactive oxygen species can stimulate proliferation, whereas antioxidant treatments can lead to late-G₁ arrest.^{40,41,49} In some cases, however, a cellular signal can cause proliferation followed by G₁/S arrest.⁵⁰

Perspectives

The study provides genome-wide insights into the mechanism of hypertension at the level of a specific nephron segment. The finding of abnormalities in cell proliferation in mTALs may stimulate a new direction of research of hypertension or hypertensive renal injury.

Acknowledgement

We thank Glenn Slocum for assistance with microscopy and image analysis and Dr Martin Hessner, Mary Kaldunski, and Shuang Jia for assistance with microarray equipment and rank-product analysis.

Sources of Funding

This work was supported by National Institutes of Health grant HL082798 and Advancing a Healthier Wisconsin Fund FP1701.

Disclosures

None.

References

1. Joe B, Letwin NE, Garrett MR, Dhindaw S, Frank B, Sultana R, Verratti K, Rapp JP, Lee NH. Transcriptional profiling with a blood pressure QTL interval-specific oligonucleotide array. *Physiol Genomics*. 2005;23:318–326.
2. Malek RL, Wang HY, Kwitek AE, Greene AS, Bhagabati N, Borchardt G, Cahill L, Currier T, Frank B, Fu X, Hasinoff M, Howe E, Letwin N, Luu TV, Saeed A, et al. Physiogenomic resources for rat models of heart, lung and blood disorders. *Nat Genet*. 2006;38:234–239.
3. Marques FZ, Campaign AE, Yang YH, Morris BJ. Meta-analysis of genome-wide gene expression differences in onset and maintenance phases of genetic hypertension. *Hypertension*. 2010;56:319–324.
4. Cowley AW Jr, Roman RJ, Kaldunski ML, Dumas P, Dickhout JG, Greene AS, Jacob HJ. Brown Norway chromosome 13 confers protection from high salt to consomic Dahl S rat. *Hypertension*. 2001;37(2 pt 2):456–461.
5. Liang M, Yuan B, Rute E, Greene AS, Zou AP, Soares P, MCQuestion GD, Slocum GR, Jacob HJ, Cowley AW Jr. Renal medullary genes in salt-sensitive hypertension: a chromosomal substitution and cDNA microarray study. *Physiol Genomics*. 2002;8:139–149.
6. Liang M, Yuan B, Rute E, Greene AS, Olivier M, Cowley AW Jr. Insights into Dahl salt-sensitive hypertension revealed by temporal patterns of renal medullary gene expression. *Physiol Genomics*. 2003;12:229–237.
7. Liang M, Lee NH, Wang H, Greene AS, Kwitek AE, Kaldunski ML, Luu TV, Frank BC, Bugenhagen S, Jacob HJ, Cowley AW Jr. Molecular networks in Dahl salt-sensitive hypertension based on transcriptome analysis of a panel of consomic rats. *Physiol Genomics*. 2008;34:54–64.
8. Lu L, Li P, Yang C, Kurth T, Misale M, Skelton M, Moreno C, Roman RJ, Greene AS, Jacob HJ, Lazar J, Liang M, Cowley AW Jr. Dynamic convergence and divergence of renal genomic and biological pathways in protection from Dahl salt-sensitive hypertension. *Physiol Genomics*. 2010;41:63–70.
9. Mori T, Polichnowski A, Glocka P, Kaldunski M, Ohsaki Y, Liang M, Cowley AW Jr. High perfusion pressure accelerates renal injury in salt-sensitive hypertension. *J Am Soc Nephrol*. 2008;19:1472–1482.
10. Tian Z, Greene AS, Usa K, Matus IR, Bauwens J, Pietrusz JL, Cowley AW Jr, Liang M. Renal regional proteomes in young Dahl salt-sensitive rats. *Hypertension*. 2008;51:899–904.
11. Liu Y, Singh RJ, Usa K, Netzel BC, Liang M. Renal medullary 11 beta-hydroxysteroid dehydrogenase type 1 in Dahl salt-sensitive hypertension. *Physiol Genomics*. 2008;36:52–58.
12. Tian Z, Liu Y, Usa K, Mladinov D, Fang Y, Ding X, Greene AS, Cowley AW Jr, Liang M. Novel role of fumarate metabolism in dahl-salt sensitive hypertension. *Hypertension*. 2009;54:255–260.
13. Liang M. Hypertension as a mitochondrial and metabolic disease. *Kidney Int*. 2011;80:15–16.
14. Alvarez-Guerra M, Garay RP. Renal Na-K-Cl cotransporter NKCC2 in Dahl salt-sensitive rats. *J Hypertens*. 2002;20:721–727.
15. Aviv A, Hollenberg NK, Weder A. Urinary potassium excretion and sodium sensitivity in blacks. *Hypertension*. 2004;43:707–713.

16. Haque MZ, Ares GR, Caceres PS, Ortiz PA. High salt differentially regulates surface NKCC2 expression in thick ascending limbs of Dahl salt-sensitive and salt-resistant rats. *Am J Physiol Renal Physiol*. 2011;300:F1096–F1104.
17. Hoagland KM, Flasch AK, Dahly-Vernon AJ, dos Santos EA, Knepper MA, Roman RJ. Elevated BSC-1 and ROMK expression in Dahl salt-sensitive rat kidneys. *Hypertension*. 2004;43:860–865.
18. Ito O, Roman RJ. Role of 20-HETE in elevating chloride transport in the thick ascending limb of Dahl SS/Jr rats. *Hypertension*. 1999;33(1 pt 2):419–423.
19. Kirchner KA. Greater loop chloride uptake contributes to blunted pressure natriuresis in Dahl salt sensitive rats. *J Am Soc Nephrol*. 1990;1:180–186.
20. Mori T, O'Connor PM, Abe M, Cowley AW Jr. Enhanced superoxide production in renal outer medulla of Dahl salt-sensitive rats reduces nitric oxide tubular-vascular cross-talk. *Hypertension*. 2007;49:1336–1341.
21. Nishi A, Eklöf AC, Bertorello AM, Aperia A. Dopamine regulation of renal Na⁺,K⁺-ATPase activity is lacking in Dahl salt-sensitive rats. *Hypertension*. 1993;21(6 pt 1):767–771.
22. Ortiz PA, Garvin JL. Intrarenal transport and vasoactive substances in hypertension. *Hypertension*. 2001;38(3 pt 2):621–624.
23. O'Connor PM, Lu L, Liang M, Cowley AW Jr. A novel amiloride-sensitive h⁺ transport pathway mediates enhanced superoxide production in thick ascending limb of salt-sensitive rats, not na⁺/h⁺ exchange. *Hypertension*. 2009;54:248–254.
24. O'Connor PM, Lu L, Schreck C, Cowley AW Jr. Enhanced amiloride-sensitive superoxide production in renal medullary thick ascending limb of Dahl salt-sensitive rats. *Am J Physiol Renal Physiol*. 2008;295:F726–F733.
25. Roman RJ, Kaldunski ML. Enhanced chloride reabsorption in the loop of Henle in Dahl salt-sensitive rats. *Hypertension*. 1991;17(6 pt 2):1018–1024.
26. Zou AP, Drummond HA, Roman RJ. Role of 20-HETE in elevating loop chloride reabsorption in Dahl SS/Jr rats. *Hypertension*. 1996;27(3 pt 2):631–635.
27. Stingo FC, Chen YA, Tadesse MG, Vannucci M. Incorporating Biological Information into Linear Models: A Bayesian Approach to the Selection of Pathways and Genes. *Ann Appl Stat*. 2011; 5: 1978–2002.
28. Trinh-Trang-Tan MM, Bouby N, Coutaud C, Bankir L. Quick isolation of rat medullary thick ascending limbs: enzymatic and metabolic characterization. *Pflugers Arch*. 1986;407:228–234.
29. Liang M, Pietrusz JL. Thiol-related genes in diabetic complications: a novel protective role for endogenous thioredoxin 2. *Arterioscler Thromb Vasc Biol*. 2007;27:77–83.
30. Moreno C, Kaldunski ML, Wang T, Roman RJ, Greene AS, Lazar J, Jacob HJ, Cowley AW Jr. Multiple blood pressure loci on rat chromosome 13 attenuate development of hypertension in the Dahl S hypertensive rat. *Physiol Genomics*. 2007;31:228–235.
31. Hartigan JA, Wong MA. A K-means clustering algorithm. *Appl Stat*. 1979;28:100–108.
32. Cheval L, Pierrat F, Dossat C, Genete M, Imbert-Teboul M, Duong Van Huyen JP, Poulain J, Wincker P, Weissenbach J, Piquemal D, Doucet A. Atlas of gene expression in the mouse kidney: new features of glomerular parietal cells. *Physiol Genomics*. 2011;43:161–173.
33. Takenaka M, Imai E, Nagasawa Y, Matsuoaka Y, Moriyama T, Kaneko T, Hori M, Kawamoto S, Okubo K. Gene expression profiles of the collecting duct in the mouse renal inner medulla. *Kidney Int*. 2000;57:19–24.
34. Virlon B, Cheval L, Buhler JM, Billon E, Doucet A, Elalouf JM. Serial microanalysis of renal transcriptomes. *Proc Natl Acad Sci USA*. 1999;96:15286–15291.
35. Yu MJ, Miller RL, Uawithya P, Rinschen MM, Khositseth S, Braucht DW, Chou CL, Pisitkun T, Nelson RD, Knepper MA. Systems-level analysis of cell-specific AQP2 gene expression in renal collecting duct. *Proc Natl Acad Sci USA*. 2009;106:2441–2446.
36. Yang L, Besschetnova TY, Brooks CR, Shah JV, Bonventre JV. Epithelial cell cycle arrest in G2/M mediates kidney fibrosis after injury. *Nat Med*. 2010;16:535–43, 1p following 143.
37. Wolf G, Ziyadeh FN, Helmchen U, Zahner G, Schroeder R, Stahl RA. ANG II is a mitogen for a murine cell line isolated from medullary thick ascending limb of Henle's loop. *Am J Physiol*. 1995;268(5 pt 2):F940–F947.
38. De Miguel C, Das S, Lund H, Mattson DL. T lymphocytes mediate hypertension and kidney damage in Dahl salt-sensitive rats. *Am J Physiol Regul Integr Comp Physiol*. 2010;298:R1136–R1142.
39. Kobori H, Nishiyama A, Abe Y, Navar LG. Enhancement of intrarenal angiotensinogen in Dahl salt-sensitive rats on high salt diet. *Hypertension*. 2003;41:592–597.
40. Dröge W. Free radicals in the physiological control of cell function. *Physiol Rev*. 2002;82:47–95.
41. Klein JA, Ackerman SL. Oxidative stress, cell cycle, neurodegeneration. *J Clin Invest* 2003; 111: 785–793.
42. Feng D, Yang C, Geurts AM, Kurth T, Liang M, Lazar J, Mattson DL, O'Connor PM, Cowley AW Jr. Increased expression of NAD(P)H oxidase subunit p67(phox) in the renal medulla contributes to excess oxidative stress and salt-sensitive hypertension. *Cell Metab*. 2012;15:201–208.
43. Taylor NE, Glocka P, Liang M, Cowley AW Jr. NADPH oxidase in the renal medulla causes oxidative stress and contributes to salt-sensitive hypertension in Dahl S rats. *Hypertension*. 2006;47:692–698.
44. Santra MK, Wajapeyee N, Green MR. F-box protein FBXO31 mediates cyclin D1 degradation to induce G1 arrest after DNA damage. *Nature*. 2009;459:722–725.
45. Tentner AR, Lee MJ, Ostheimer GJ, Samson LD, Lauffenburger DA, Yaffe MB. Combined experimental and computational analysis of DNA damage signaling reveals context-dependent roles for Erk in apoptosis and G1/S arrest after genotoxic stress. *Mol Syst Biol*. 2012;8:568.
46. Ying WZ, Wang PX, Sanders PW. Induction of apoptosis during development of hypertensive nephrosclerosis. *Kidney Int*. 2000;58:2007–2017.
47. Mattson DL, James L, Berdan EA, Meister CJ. Immune suppression attenuates hypertension and renal disease in the Dahl salt-sensitive rat. *Hypertension*. 2006;48:149–156.
48. Penzo M, Massa PE, Olivetto E, Bianchi F, Borzi RM, Hanidu A, Li X, Li J, Marcu KB. Sustained NF- κ B activation produces a short-term cell proliferation block in conjunction with repressing effectors of cell cycle progression controlled by E2F or FoxM1. *J Cell Physiol*. 2009;218:215–227.
49. Havens CG, Ho A, Yoshioka N, Dowdy SF. Regulation of late G1/S phase transition and APC Cdh1 by reactive oxygen species. *Mol Cell Biol*. 2006;26:4701–4711.
50. Shimi T, Butin-Israeli V, Adam SA, Hamanaka RB, Goldman AE, Lucas CA, Shumaker DK, Kosak ST, Chandel NS, Goldman RD. The role of nuclear lamin B1 in cell proliferation and senescence. *Genes Dev*. 2011;25:2579–2593.

Novelty and Significance

What Is New?

- Novel and unexpected findings on changes in cell proliferation in medullary thick ascending limbs.
- One of the first studies to examine the transcriptome in tissues highly enriched for a single cell type in hypertension.
- Application of a Bayesian method to hypertension research to identify biological pathways independent of determination of differential expression.

What Is Relevant?

- The study provides genome-wide insights into the mechanism of hypertension at the level of a specific nephron segment.

Summary

We identified several biological pathways in the mTAL that might contribute to hypertension or hypertensive renal injury and provided novel evidence for alterations in cell proliferation in medullary thick ascending limbs in salt-sensitive rats.